2012

Improved photovoltaic performance of dye-sensitized solar cells with modified self-assembling highly ordered mesoporous TiO2 photoanodes

Ziqi Sun
University of Wollongong, ziqi@uow.edu.au

Jung Ho Kim
University of Wollongong, jhk@uow.edu.au

Yue Zhao
University of Wollongong, yue@uow.edu.au

Fargol Bijarbooneh
University Of Wollongong, uow@bijarbooneh.edu.au

Victor Malgras
University of Wollongong, vm961@uowmail.edu.au

See next page for additional authors

Improved photovoltaic performance of dye-sensitized solar cells with modified self-assembling highly ordered mesoporous TiO2 photoanodes

Abstract

Strategies for improving the photovoltaic performance of dye-sensitized solar cells (DSSCs) are proposed by modifying highly transparent and highly ordered multilayer mesoporous TiO2 photoanodes through nitrogen-doping and top-coating with a light-scattering layer. The mesoporous TiO2 photoanodes were fabricated by an evaporation-induced self-assembly method. In regard to the modification methods, the light-scattering layer as a top-coating was proved to be superior to nitrogen-doping in enhancing not only the power conversion efficiency but also the fill factor of DSSCs. The optimized bifunctional photoanode consisted of a 30-layer mesoporous TiO2 thin film (4.15 mm) and a Degussa P25 light-scattering top-layer (4 mm), which gives rise to a similar to 200% higher cell efficiency than for unmodified cells and a fill factor of 0.72. These advantages are attributed to its higher dye adsorption, better light scattering, and faster photon-electron transport. Such a photoanode configuration provides an efficient way to enhance the energy conversion efficiency of DSSCs.

Keywords

tio2, mesoporous, ordered, highly, assembling, self, photoanodes, modified, improved, cells, solar, sensitized, dye, performance, photovoltaic

Disciplines

Engineering | Physical Sciences and Mathematics

Publication Details

Sun, Z., Kim, J., Zhao, Y., Bijarbooneh, F., Malgras, V. & Dou, S. Xue. (2012). Improved photovoltaic performance of dye-sensitized solar cells with modified self-assembling highly ordered mesoporous TiO2 photoanodes. Journal of Materials Chemistry, 22 (23), 11711-11719.

Authors

Ziqi Sun, Jung Ho Kim, Yue Zhao, Fargol Bijarbooneh, Victor Malgras, and S X. Dou

Journal Name

Dynamic Article Links ►

Cite this: DOI: 10.1039/c0xx00000x

www.rsc.org/xxxxxx

ARTICLE TYPE

Improved Photovoltaic Performance of Dye-sensitized Solar Cells with Modified Self-assembly Highly Ordered Mesoporous TiO_2 Photoanodes

Ziqi Sun[a], Jung Ho Kim*[a], Yue Zhao[a], Fargol Bijarbooneh[a], Victor Malgras[a], Shi Xue Dou[a]

Received (in XXX, XXX) Xth XXXXXXXXX 20XX, Accepted Xth XXXXXXXXX 20XX

DOI: 10.1039/b000000x

Strategies for improving the photovoltaic performance of dye-sensitized solar cells (DSSCs) are proposed by modifying highly-transparent and highly-ordered multilayer mesoporous TiO_2 photoanodes through nitrogen-doping and top-coating with a light-scattering layer. The mesoporous TiO_2 photoanodes were fabricated by an evaporation-induced self-assembly method. In regard to the modification methods, the light-scattering layer as a top-coating was proved to be superior to nitrogen-doping in enhancing not only the power conversion efficiency, but also the fill factor of DSSCs. The optimized bifunctional photoanode consisted of a 30-layer mesoporous TiO_2 thin film (4.15 μm) and a Degussa P25 light-scattering top-layer (4 μm), which gives rise to a ~200% higher cell efficiency than for unmodified cells and a fill factor of 0.72. These advantages are attributed to its higher dye adsorption, better light scattering, and faster photon/electron transport. Such a photoanode configuration provides an efficient way to enhance the energy conversion efficiency of DSSCs.

Introduction

In recent years, soaring fossil fuel prices have driven up the demand for economically renewable energy sources more than ever. Solar energy, one of the greenest power sources with near zero CO_2 emission, provides an efficient and sustainable solution to resolve the energy crisis. Despite widespread commercialization of silicon based solar cells, the dye-sensitized solar cell (DSSC) is emerging as a strong potential candidate for next generation solar energy devices.[1, 2] The basic concept of the DSSC involves the high porosity of nanostructured TiO_2 film, enabling a large concentration of sensitizing organic dye to be adsorbed. The adsorbed dye-molecules are capable of absorbing light and injecting electrons into the TiO_2 conduction band. The electrons are then collected at a back conducting electrode, generating a photocurrent. Therefore, one of the key issues for superior DSSCs is the morphological engineering of the TiO_2 photoanode.[1-4] It is well-accepted that a highly efficient photoanode for DSSCs requires not only a high surface area for a large amount of dye molecule loading, but also an optimum construction for light harvesting and fast electron transport without dissipation.[5-8]

Recently, mesoporous oxide materials with a highly ordered channel/matrix structure have received extensive attention. Mesoporous TiO_2 film patterned on conductive transparent glass, which features a highly-ordered mesochannel structure and high specific surface area, can improve the performance of photovoltaic cells when it is applied as photoanode. Zukalova *et al.* fabricated 1 μm-thick highly-ordered mesoporous TiO_2 photoanode with pore size of about 6 nm using an amphiphilic triblock copolymer of ethylene oxide and propylene oxide as template.[9] The obtained power conversion efficiency of the DSSCs was up to 4.0%, which was about 50% higher than the outcome using standard mesoporous TiO_2 films with the same film thickness (2.7%).[9] Hou *et al.* also reported a solar conversion efficiency of 5.31% using 2.5 μm-thick wormlike mesoporous TiO_2 film as photoanode.[10]

Even though the highly-ordered TiO_2 thin film has a well-controlled mesoporous structure, narrow pore size distribution, and high specific surface area, it is difficult to reach a thickness above 4 μm by the conventional self-assembly method.[11] Consequently, further improvement in cell performance is limited by the thinness of the mesoporous TiO_2 film, resulting in less dye up-take. From reports in the literature, in order to obtain mesoporous TiO_2 films more than 1 μm thick, dip-coating, self-assembly, and precalcination procedures had to be repeated many times.[9-10] However, the repeated procedures will result in an opaque film with degraded mesostructure. Wei *et al.* prepared a mesoporous TiO_2 photoanode 20 μm in thickness by screen printing prepared mesoporous TiO_2 powders made with Pluronic P123 template,[12] but the mesoporous structure only showed short-range order in this case. The randomly arranged nanochannels on the macroscale would offset the merit of fast photon/electron transportation that is featured in highly-ordered mesoporous photoanode. Hence, for taking advantage of highly-ordered mesoporous TiO_2 photoanode, strategic modifications to conquer its intrinsic thinness due to the self-assembly method are necessary for superior DSSCs.

An advanced synthetic approach for fabricating highly-ordered mesoporous thin film is the evaporation induced self-assembly (EISA) process, which offers a unique combination of controllable nanoscale architecture, material variation and low-

cost solution processing. A dilute, usually acidic, solution of inorganic precursor and an amphiphilic organic template is produced in a volatile solvent containing some water. The solution is spin- or dip-coated onto virtually any substrate. On evaporation of the organic solvent, the system self-organizes to form a periodic inorganic–organic composite. Thermal treatment can be used to further crosslink the inorganic framework and remove the organic template, producing a nanoporous thin film. This method allows the fabrication of uniform thin films with highly ordered nanochannels over large areas.[13-16]

In this study, by using the EISA method, we firstly prepared highly-transparent and highly-ordered mesoporous TiO_2 thin films by tuning surfactants and coating layers. It is expected that the highly ordered nanochannels within the thin films will allow the fast transport of photons and electrons. To overcome the low-efficiency resulting from the thinness of the EISA TiO_2 photoanodes, strategies of nitrogen-doping (N-doping) and top-coating with a light-scattering layer were further adopted. Finally, a comparative study was carried out in detail to examine the validity of these approaches.

Experimental

Preparation of TiO_2 mesoporous photoanodes

For the preparation of highly-ordered mesoporous TiO_2 films, 1.05 g titanium isopropoxide (TTIP, Sigma-Aldrich) was hydrolyzed by adding 0.74 g HCl after stirring for 10 min at room temperature. The hydrolyzed sol was then mixed with either 0.2 g Pluronic P123 (Sigma-Aldrich) or 0.35 g Pluronic F127 (Sigma-Aldrich) dissolved in 3.00 g ethanol and stirred for 15 min at room temperature. The resulting solution was spin-coated on pieces of fluorine-doped tin oxide (SnO_2:F, FTO) transparent glass (7 Ω/sq, Pilkington TEC Glass™) with an area of 20 × 20 mm^2 at a rate of 4000 rpm for 30 seconds, followed by air aging for 2 days at 25 ^oC under humidity of 45-55%. For the preparation of multilayer TiO_2 thin film through spin coating, the upper layer was recoated after the former layer was dried on a 60 ^oC plate heater for 30 min. The numbers of layers were set at 5, 10, 15, 20, and 30. The multilayer TiO_2 coatings were also aged under the same conditions as for the preparation of single-layer thin films. All samples were finally calcined in a tube furnace at 400 ^oC for 6 h with a heating/cooling rate of 2 ^oC/min to remove the surfactants.

Nitrogen-doping of TiO_2 mesoporous photoanodes

A simple direct nitridation was carried out to modify the band structure of mesoporous TiO_2 thin film by N-doping. In detail, 3.00 g urea was loaded on the prepared TiO_2 thin films in covered Al_2O_3 boats, which were then heated to 500 ^oC for 5 hours under an Ar atmosphere. After the thermal treatment, the surface of the films was rinsed with distilled water or diluted hydrochloric acid solution to remove residual urea and its by-products.

Top-coating light-scattering layer on TiO_2 mesoporous photoanodes

Degussa P25 TiO_2 (Sigma-Aldrich) nanoparticles around 20 nm in diameter were coated on the top of multilayer TiO_2 mesoporous film as a scattering layer. Firstly, a Degussa P25 TiO_2 nanoparticle slurry was prepared by mixing with ethanol and dispersants. Then, the well-dispersed P25 slurry was coated onto the highly-ordered mesoporous TiO_2 thin film by applying the doctor-blade method. The thickness of the as-prepared green film was controlled at 40 μm. After heating at 400 ^oC for 1 h, the actual scattering layer became thinner, around 4 μm.

Assembly of dye-sensitized solar cells

Dye adsorption was carried out by immersing the highly-ordered mesoporous TiO_2 thin films in ethanol-based commercial N719 (Sigma-Aldrich) dye solution at 25 ^oC for 24 h. The solar cells were prepared by assembling a Pt counter electrode and a dye-adsorbed mesoporous TiO_2 photoanode, and then sealed by using a Surlyn (Dupont) thermoplastic frame (25 μm thick). A commercial electrolyte purchased from Solaronix (Iodolyte AN-50, Switzerland) was poured into the electrode, and the cell was then sealed again.

Characterization

The phase composition of mesoporous thin films was identified by X-ray diffraction (XRD, GBC Scientific Equipment, Hampshire IL, USA) and Raman spectroscopy (LabRam-HR 800, HORIBA JOBIN YVON, Longjumeau Cedex, France). Coating morphology was observed via a scanning electron microscope (SEM, JEOL-6700F, Tokyo, Japan) and a 200 kV transmission electronic microscope (TEM, JEOL-2011F, Tokyo, Japan). The absorption spectra of thin films were obtained using an ultraviolet-visible (UV-Vis) spectrometer (Perkin-Elmer, Wellesley MA, USA). For the nitrogen-doped specimens, the chemical state was identified by using an X-ray photoelectron spectrometer (XPS, ESCALAB250, VG) with monochromatized Al K_α X-ray radiation (1486.6 eV). All measurements were performed under an ultra-high vacuum on the order of 10^{-8} Pa. In each case a neutralizer was used to eliminate the charge effect, which occurs in non-conducting samples. The binding energy was determined with reference to the C 1s line at 284.6 eV of adventitious carbon. The photocurrent density-voltage (*J*-*V*) characteristic was measured by exposing the cell to air mass (AM) 1.5 simulated sunlight from a solar simulator (PEL-L12, Peccell Technologies, Japan) combined with a Keithley 2400 source meter. Incident-photon-to-current quantum conversion efficiency (IPCE) was measured as a reference spectrum, using an optical fibre (3 mm diameter) for monochromatic irradiation (PEC-S20DC, Peccell Technologies, Japan). Monochromatic photocurrent was monitored by the continuous irradiation (dc measurement) method.

Results and discussion

Mesoporous thin film preparation

The highly-ordered mesoporous TiO_2 thin films were successfully fabricated via the evaporation-induced self-assembly (EISA) method by using either Pluronic P123 or F127 as surfactant (with such samples hereafter designated as P123 and F127, respectively). Fig. 1(a) and (b) presents top-view SEM images of the single layer TiO_2 thin films with different surfactants. We observed that well-ordered mesoporous structures were obtained with an average pore size of 13 nm and 10 nm, respectively, for P123 and F127, along with an average wall thickness of around 10 nm for both samples, by analyzing the

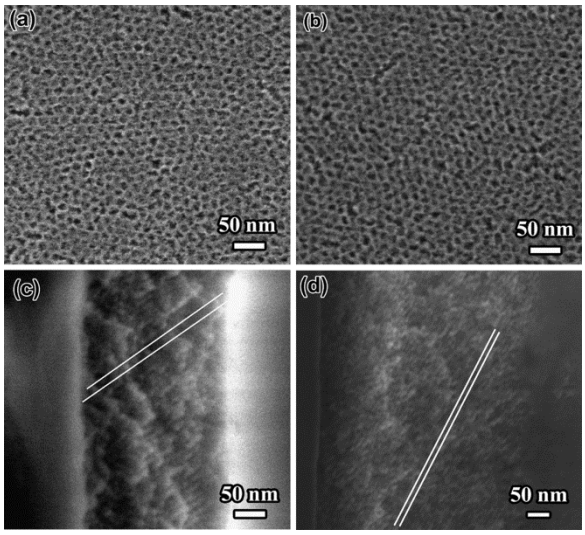

Figure 1: SEM images of the top surfaces of mesoporous TiO_2 thin films synthesized from (a) P123 template and (b) F127 template; and the corresponding cross-sectional images of the thin films synthesized from (c) P123 template and (d) F127 template.

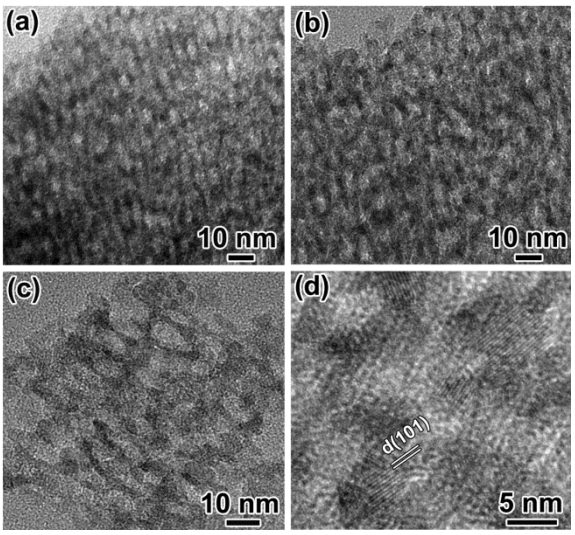

Figure 2: Transmission electron cross-sectional micrographs of the highly-ordered mesoporous TiO_2 thin films fabricated with the surfactants (a) P123 and (b) F127; (c) a high-magnification image of (b), and (d) a HRTEM image of the TiO_2 matrix.

SEM top-surface images. It is worth noting that there was a noticeable difference in the film thickness of these two samples, where the corresponding thicknesses were 245 nm and 490 nm, respectively, for P123 and F127. Cross-sectional images of single layer mesoporous thin films are also shown in Fig. 1(c) and (d), where the nanochannels that pass through the films can be distinguished. The highly-ordered channels could improve optical absorption, which has benefits for fast photon/electron transportation. Owing to the presence of open nanochannels and the nanomatrix, the prepared mesoporous thin films are expected to be characterized by high specific surface area, highly efficient dye uptake and a rapid photo-electro redox reaction between dye and electrolyte, thus enhancing the overall performance of the DSSCs.

The mesostructure of the obtained thin films was further characterized by TEM. Fig. 2(a) and (b) presents cross-sectional TEM images of the nanochannels obtained from P123 and F127 templates, respectively. They provide direct observation of the highly ordered mesoporous networks and periodicity. The high magnification image in Fig. 2(c) demonstrates that the walls of the nanochannels are in the range of 3-5 nm. Fig. 2(d) shows a high-resolution TEM (HRTEM) image of the highly-ordered matrix, which demonstrates that the TiO_2 obtained by this EISA method should be in anatase phase with crystalline size around 3-5 nm.

According to previous studies, highly-ordered mesoporous thin film for DSSCs performed much better than Degussa P25 TiO_2 solar cells with the same film thickness.[9, 10, 17] However, in the former case, the small amount of dye adsorbed by the lesser thickness of the mesoporous film is a major bottleneck for increasing the power conversion efficiency of the solar cells. Herein, multilayer mesoporous TiO_2 thin films were prepared by repeated spin coating with the aim of adsorbing a large amount of dye. To obtain a highly-transparent thin film, the coating repetition rate was controlled within 30 times. Fig. 3(a) presents the change in the thickness of the multilayer mesoporous thin film as a function of coating times. We note that the thickness increased to 4.15 and 5.85 μm, respectively, for up to 30 coating layers for samples P123 and F127. The insets in Fig. 3(a) display the low and high magnification cross-sectional images of the 30-layer P123 film after calcination, which still maintained the highly-ordered mesoporous structure. After removing the P123 or F127 surfactant, highly-transparent, smooth, and intact TiO_2 thin films were obtained on the FTO substrates. For the sake of comparison, highly-transparent photoanode made from Solaronix TiO_2 (Ti-Nanoxide HT/SP) paste with a thickness of 1.13 μm was also prepared using the doctor-blade method.

Fig. 3(b) shows the UV-Vis spectra of mesoporous thin films with different layer numbers together with the Solaronix thin film. The absorbance onsets of the mesoporous TiO_2 thin films over 10 layers were at around 350 nm and the corresponding band gap was around 3.55 eV (inset in Fig. 3(b)), which shows an obvious

'blue-shift' compared with Solaronix TiO_2 and bulk anatase TiO_2. The reported band gap of bulk anatase TiO_2 is around 3.25 eV (with the absorbance onset around 380 nm).[4] The band structure of TiO_2 with different particle sizes has been studied.[18] The results showed that the particle size on the nanoscale raises the conduction band and lowers the valence band. The widened band gap is displayed as a blue shift of the absorbance edge in UV-Vis absorption spectra. The blue shift in our case, therefore, can be attributed to the small size of the anatase nanocrystallites in the mesoporous thin film. At the same time, the coating thickness was observed to slightly influence the band gap as well. The absorbance edge of the 5-layer thin film exhibited a smaller blue shift compared to the thicker ones. The highly-transparent Solaronix thin film has a narrower band gap (around 3.45 eV) compared to the mesoporous thin films, but it is still wider than for bulk anatase. The variation in the band gap will, in turn, affect the interband excitation of the photoanode in the UV light regime and the open-circuit photovoltage of the cells.

A detailed phase composition analysis of the mesoporous TiO_2

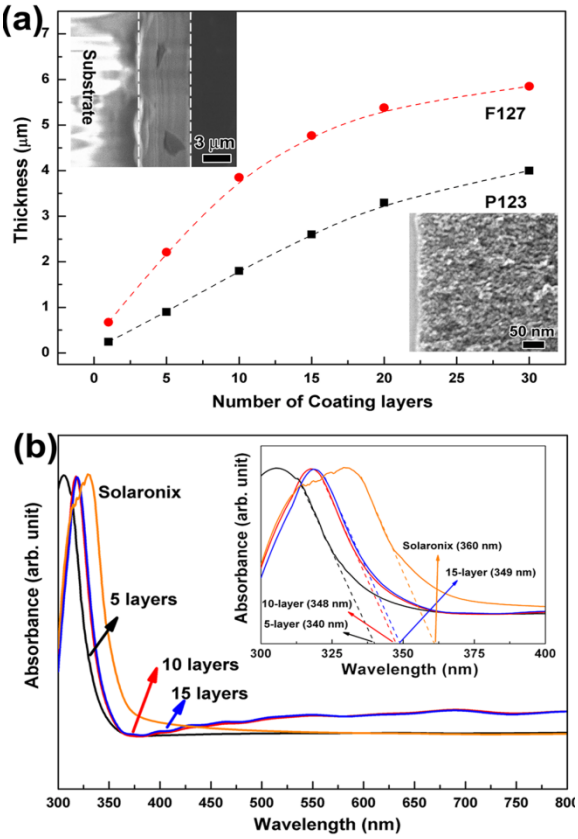

Figure 3: (a) Thickness of P123 and F127-templated mesoporous TiO_2 thin films as a function of number of coatings, with the inset presenting the low and high magnification cross-sectional images of a 30-layer P123-templated mesoporous thin film; and (b) UV-Vis spectra of P123-templated mesoporous TiO_2 thin films, with the inset showing an enlargement of the low wavenumber range.

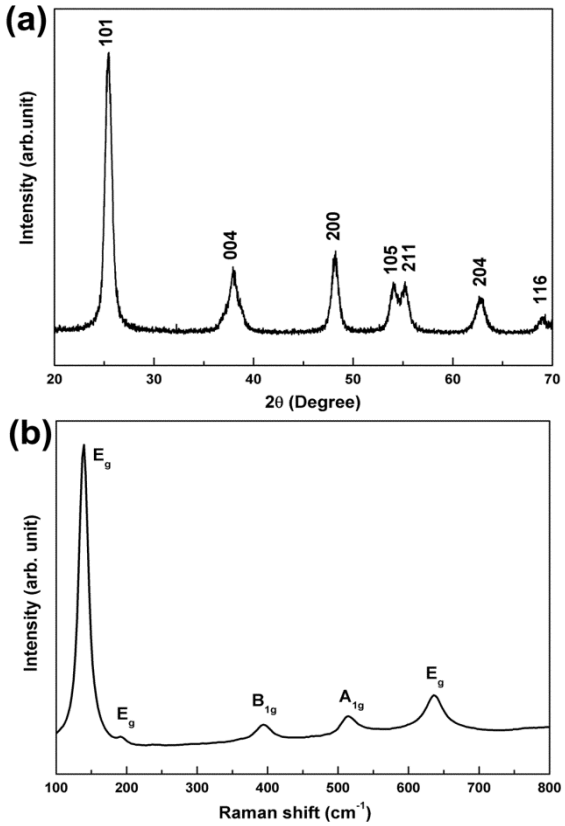

Figure 4: Typical (a) XRD and (b) surface Raman spectra collected from the mesoporous TiO_2 thin films.

thin films is shown in Fig. 4. Very clear peaks of anatase TiO_2 were observed from the XRD patterns (Fig 4(a)). Raman scattering results also show that the detected vibration bands are related to only anatase TiO_2 phase, as shown in Fig. 4(b). Three E_g modes centred at around 144, 196, and 640 cm^{-1}, and two B_{1g} modes at 398 and 519 cm^{-1} can be assigned to the Raman active fundamental vibrations of anatase TiO_2.[19]

Photovoltaic performance measurements

Performance of solar cells with highly-ordered mesoporous TiO_2 photoanode

Photovoltaic performances of the highly-ordered mesoporous TiO_2 photoanodes made from P123 were tested under simulated sunlight. The Solaronix TiO_2 photoanode was also measured as a reference. The summarized results on short-circuit current density (J_{sc}), open-circuit voltage (V_{oc}), fill factor (F), and power conversion efficiency (η), are tabulated in Table 1. Fig. 5(a) shows the photocurrent density - photovoltage (J-V) curves of the solar cells with highly-ordered TiO_2 mesoporous photoanodes with different numbers of coating layers. We observed that the photocurrent density increased as the TiO_2 film thickness increased. For instance, the J_{sc} increased from 0.92 $mA{\cdot}cm^{-2}$ for the 5-layer photoanode to 4.15 $mA{\cdot}cm^{-2}$ for the 30-layer one. The values of V_{oc} of the mesoporous photoanode cells slightly varied around 0.8 V, which is higher than the 0.6-0.7 V for some

Table 1: Photovoltaic performances (short-circuit current density J_{sc}, open-circuit voltage V_{oc}, fill factor F and conversion efficiency η) of solar cells with highly-transparent photoanodes consisting of Solaronix TiO_2 nanoparticles and highly-ordered multilayer mesoporous TiO_2 thin films.

Photoanodes	Thickness (μm)	J_{sc} ($mA{\cdot}cm^{-2}$)	V_{oc} (V)	F	η (%)
Solaronix	1.13	0.58	0.65	0.43	0.16
P123-5 layer	0.92	1.64	0.80	0.62	0.82
P123-10layer	1.80	3.09	0.78	0.58	1.40
P123-15layer	2.65	4.38	0.83	0.50	1.82
P123-30layer	4.15	5.47	0.77	0.57	2.40
F127-30layer	5.85	4.26	0.79	0.56	1.86

reported nanoparticle TiO_2 cells.[2, 7] As a result of the widened band gap of mesoporous TiO_2 photoanodes demonstrated by the UV-Vis spectra, there was a higher conduction band gap energy and a higher Fermi level for the mesoporous photoanodes, and thus an increased photovoltage, V_{oc}, of the solar cells.[2]

It is worth noting that both the J_{sc} and the V_{oc} of the highly-ordered mesoporous TiO_2 thin film solar cells had higher values than for the the Solaronix one with similar thickness (Table 1). For example, the 5-layer coated TiO_2 photoanode 0.9 μm in thickness had a J_{sc} of 1.64 $mA{\cdot}cm^{-2}$ and a V_{oc} of 0.80 V, while for the Solaronix photoanode 1.13 μm in thickness, they were 0.58 $mA{\cdot}cm^{-2}$ and 0.65 V, respectively. What most important is that the energy conversion efficiency (η) of the 5-layer thin film solar cell was 0.82%, 5 times higher than that of the Solaronix

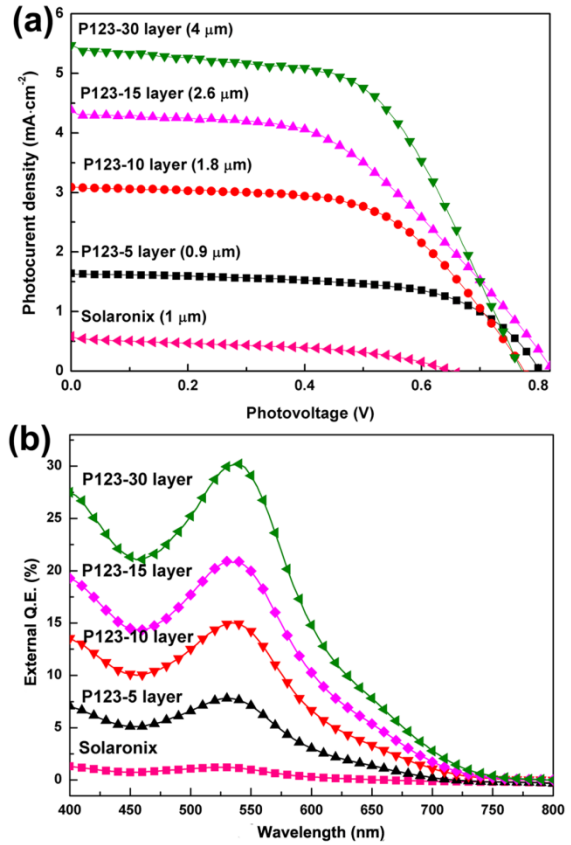

Figure 5: (a) Photocurrent-photovoltage (*J-V*) curves and (b) incident-photon-to-current conversion efficiency (IPCE) spectra of the solar cells with photoanodes consisting of P123-templated mesoporous TiO_2 thin films and Solaronix TiO_2 nanoparticle thin film.

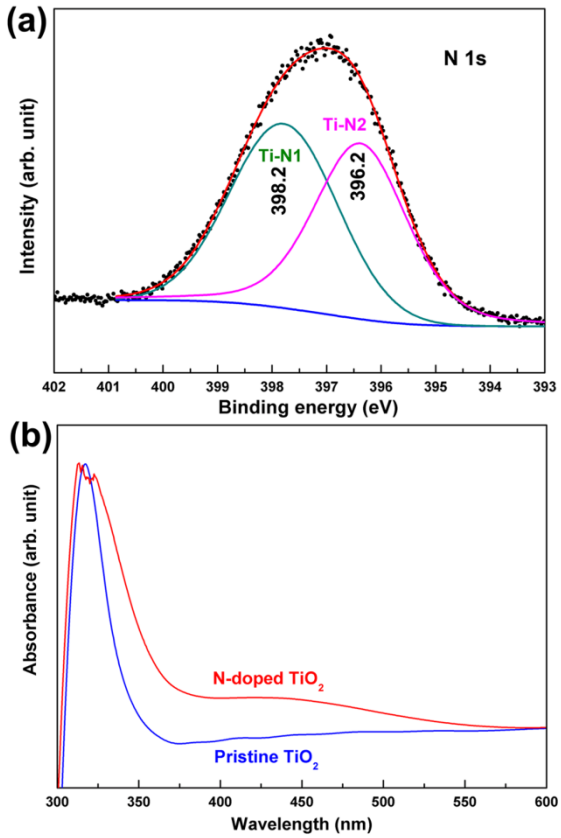

Figure 6: (a) Fitted N 1s XPS spectrum and (b) UV-Vis spectra of N-doped and undoped mesoporous TiO_2 thin films.

cell (0.16%). One of the biggest differences between the highly-ordered TiO_2 mesoporous photoanode and the Solaronix one is the presence of highly-aligned nanochannels in the matrix of the former. The performance gap between these two kinds of photoanodes confirms the importance of fast photon/electron transport pathways for improving the cell efficiency.

The improvement of J_{sc} in the highly-ordered mesoporous TiO_2 photoanodes can be attributed to the increased injection of electrons and the improved charge-transfer capability.[20] The highly-transparent and highly-ordered TiO_2 photoanode features very fine porous channels and nanoparticle walls, and thus a high amount of semiconductor - dye - electrolyte interfacial areas. As a consequence, the highly-ordered anodes can adsorb a large proportion of dye on the electrode and allow fast transportation of photons and electrons along the channels and walls. The high J_{sc} also indicates that the electron-hole recombination reaction is inhibited at the TiO_2/dye/electrolyte interfaces.[21] Therefore, owing to the higher dye loading on the photoanode and the faster charge transfer ability, as well as retarded electron-hole recombination, the highly-ordered mesoporous TiO_2 thin film solar cells exhibited superior photon-electron conversion efficiency, e.g., for the solar cell with the 30-layer highly-ordered thin film anode, the conversion efficiency was up to 2.40%.

The photoactive wavelength regime for the mesoporous thin film solar cells and Solaronix nanoparticle solar cells was evaluated by IPCE spectra, as shown in Fig. 5(b). Two excitonic peaks can be observed in the active spectra for all tested samples. One of the peaks in the wavelength range of 400-500 nm originates from the excitation from the top of the valence band to the bottom of the conduction band in TiO_2 under UV light.[22] The external quantum efficiencies (QEs) of the P123-templated mesoporous TiO_2 photoanodes in this wavelength range increased significantly with increasing film thickness, which coincides well with the increasing amount of TiO_2 in the photoanodes. Another peak in the IPCE spectra was located in the visible light range of 450-700 nm. The intensity of these peaks also showed a strong correlation with the multilayer thickness. It has been reported that the excitation of DSSCs in the wavelength range of 450-700 nm is aroused by the injection of electrons from the dye to the TiO_2 photoanode.[22] Therefore, the enhancement of IPCE in the 450-700 nm range as a function of increased mesoporous TiO_2 thin film thickness reflects the increased dye uptake amount in the photoanode. In other words, the thicker the mesoporous thin film is, the higher the dye loading in the photoanodes.

As shown in Table 1, the maximum cell efficiency of the photoanodes made from sample F127 was only 1.86%, lower than for those made from sample P123, 2.40%, even if the F127-templated TiO_2 thin film was thicker. This phenomenon might be interpreted from the fact that the nanochannels in the F127 thin film were more inclined towards the FTO substrate, i.e., the larger the angle between the nanochannels and the light incident direction is, the less efficient the absorption/transportation of photons from the perpendicular incident sunlight. Another

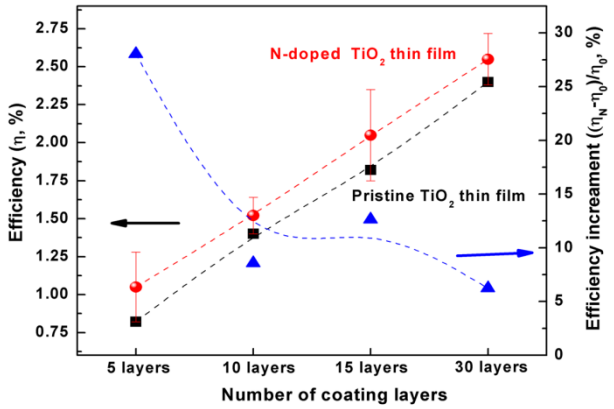

Figure 7: Photoconversion efficiency and efficiency enhancement of solar cells with N-doped mesoporous TiO_2 thin films photoanodes.

possibility is the smaller nanochannels in the F127 film than those in the P123 film (Fig. 2 (c-d)), which may retard full dye uptake. In the following sections, we will mainly discuss the mesoporous TiO_2 photoanodes made from P123 surfactant.

Even though a dramatic enhancement of the solar cell energy conversion efficiency was achieved by employing highly-ordered mesoporous TiO_2 thin films as efficient photoanodes, further improvement to realize commercialization is still restricted by the relative thinness of the TiO_2 films. Thus, strategies to enhance the performance of highly-ordered mesoporous TiO_2 thin film solar cells need to be addressed.

Performance of solar cells with N-doped mesoporous TiO_2 photoanodes

The efficiency of TiO_2 nanocrystalline film based DSSCs is low because it is limited by poor light harvesting due to the shortage of optical elements in electrode films. One way to enhance the photocapture efficiency and optical absorption of photoelectrode films is introducing non-metallic doping into TiO_2 nanostructures. The non-metallic doping is helpful for enhancing the visible light absorption and photocurrent generation in photoanodes.[23-26] Nitrogen doped TiO_2 nanocrystalline photoanode has shown enhanced photocatalytic activity under visible light irradiation and improved stability in operation.[25-27]

Fig. 6(a) presents the XPS spectrum of the N 1s core level obtained from the azotized TiO_2 thin film. Here, the deconvolution peaks in the N 1s XPS spectrum are at 398.2 and 396.2 eV, respectively. There is still controversy concerning the assignment of the peak feature in XPS for the nitrogen-doped TiO_2. For example, Burda *et al.* observed a peak centered at 401.3 eV and assigned it to the N substitution for O in the lattice,[22] while Ma *et al.* pointed out that the peak around 400 eV was likely to have originated from the molecularly adsorbed nitrogen species.[27] Concerning other peaks, Asahi *et al.* reported that the peak around 396 eV in the N 1s spectra was derived from the substitutional N in TiO_2, corresponding to Ti-N-Ti bonding.[28] They also found that the visible light photocatalytic activity increased with the intensity of the 396 eV peak in the N 1s XPS spectra, so that the substitution of N in O sites contributes to the improvement in the visible light activity of TiO_2.[28] This result has been accepted by other researchers.[29-30] As for the peak at 398

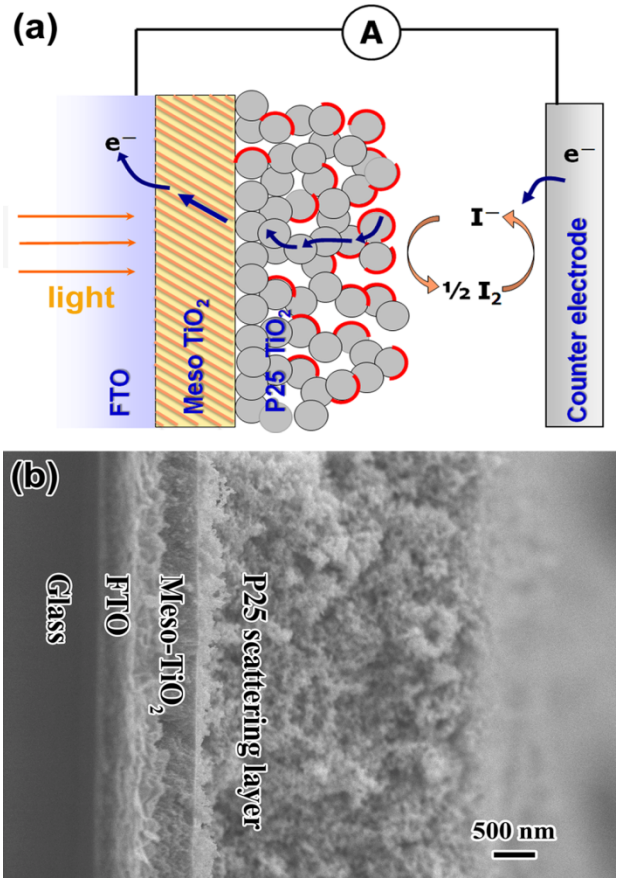

Figure 8: (a) Schematic diagram of a DSSC with bifunctional photoanode consisting of a highly-ordered mesoporous thin film and a scattering layer, and (b) cross-sectional SEM image of a bifunctional photoanode consisting of a 5-layer highly-ordered TiO_2 mesoporous thin film and a 4 μm P25 nanoparticle scattering layer.

eV, Ma *et al.* assigned it to the partial substitution of O-Ti-O by N, or the O-Ti-N structure.[27] However, Zhou *et al.* suggested that the 398 eV peak should be attributed to the invasion of N atoms into the interstitial sites of the TiO_2 crystal lattice, expressed as the Ti-N-O bond, and this conclusion was confirmed by a temperature programmed desorption (TPD) experiment.[31] In our study, the absence of any peak around 400 eV in the N 1s spectrum implies that there were no adsorbed nitrogen molecules in our samples. Based on the most accepted results, the peak at 398.2 eV, which is marked as Ti-N1in Fig. 6(a), can be interpreted as the result of N atoms occupying the interstitial sites of the TiO_2 lattice (Ti-N_i-O). The peak at 396.2 eV labelled as Ti-N2, could be derived from the substitution of N on the oxygen sites in TiO_2 (O-Ti-N_s). By comparing the integral areas of the N 1s peaks, there is evidence that the quantity of N atoms occupying the open interstitial sites was much greater than that of those substituting into O sites in the mesoporous thin films after direct nitridation treatment.

The successful N-doping in TiO_2 photoanodes also can be easily visualized from the surface colour change of the thin films from transparent to light yellow, which correlates with the varied optical response in the visible wavelength range. Fig. 6(b) presents the UV-Vis absorption spectra of the N-doped and

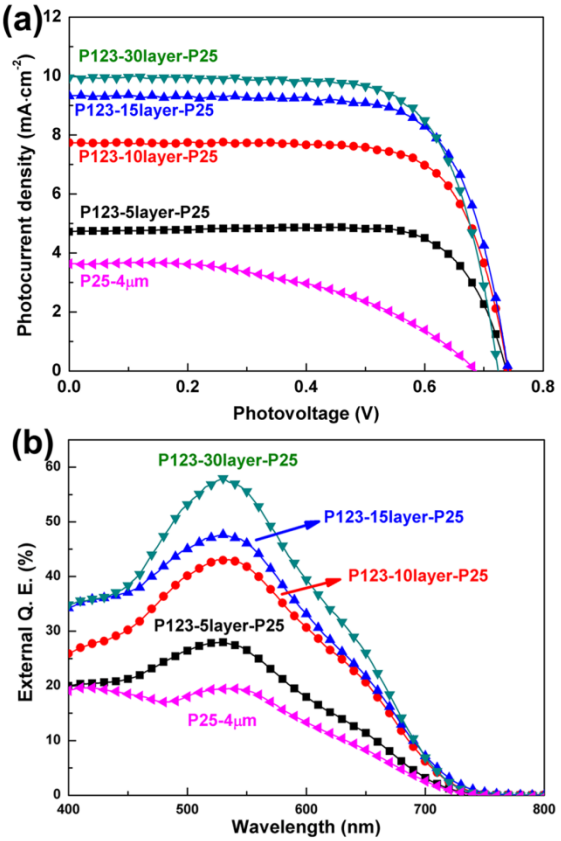

Figure 9: (a) Photocurrent-photovoltage (*J*-*V*) curves and (b) incident-photon-to-current conversion efficiency (IPCE) spectra of the solar cells with bifunctional photoanodes or single-layer P25 nanoparticle photoanode.

pristine TiO_2 thin film. The absorbance onsets in Fig. 6(b) shift from 350 nm to 390 nm after N-doping, indicating that the band-gap of TiO_2 becomes narrower, from 3.55 eV to 3.19 eV. This result agrees well with the results reported by Asahi *et al.*, who also observed the band-gap narrowing of N-doped TiO_2 thin films and proposed that the narrowed band gap is caused by the hybridization of the dopant N 2p state with the O 2p valence band in TiO_2.[23] Furthermore, the N-doped TiO_2 thin film exhibited a new absorbance peak in the 400-550 nm wavelength region. It was considered to have arisen from a new state lying close to the valence band edge as a result of nitrogen doping.[27]

Fig. 7 compares the energy conversion efficiency of the solar cells containing N-doped and pristine mesoporous TiO_2 photoanodes, respectively. The N-doped 5-layer mesoporous thin film photoanode exhibited an enhancement of 30% in solar energy conversion efficiency compared to the undoped one. However, this increment was fixed at around 10% when TiO_2 multilayers go beyond 5 layers. The highest conversion efficiency achieved in the present study was 2.55% for the N-doped 30-layer mesoporous photoanode. The lesser conversion efficiency growth with increasing thickness of the N-doped photoanodes may be due to a reduction of the nitrogen doping effect with depth in the TiO_2 thin film. If we consider the error bars for the efficiency of N-doped solar cells, the enhancement of photovoltaic performance of the mesoporous TiO_2 solar cells by N-doping is not as significant as we expected.

Table 2: Photovoltaic performances (short-circuit current density J_{sc}, open-circuit voltage V_{oc}, fill factor F, and conversion efficiency η) of solar cells with bifunctional photoanode consisting of a highly-ordered multilayer mesoporous TiO_2 thin film and a 4-μm Degussa P25 TiO_2 light-scattering layer, and of a cell with single-layer 4-μm Degussa P25 TiO_2 photoanode only.

Photoanodes	J_{sc} (mA·cm^{-2})	V_{oc} (V)	F	η (%)
P123-5 layer-P25	4.72	0.74	0.78	2.70
P123-10 layer-P25	7.74	0.74	0.73	4.19
P123-15 layer-P25	9.32	0.74	0.72	4.98
P123-30 layer-P25	9.95	0.72	0.72	5.18
P25-4 μm	6.36	0.48	0.35	1.07

Performance of solar cells with bifunctional mesoporous TiO_2 photoanode

An alternative way to enhance photocapture efficiency and optical absorption of photoelectrode films is to introduce an efficient light-scattering layer by top-coating.[32] Many research groups have succeeded in improving the efficiency of TiO_2-based DSSCs by introducing light-scatterers.[32-35] As reported by Qiu *et al.*, a double-layered photoanode made from variable-size anatase TiO_2 nanospindles not only had high specific surface area, but also showed stronger aggregation-induced light scattering in the visible wavelengths of the solar spectrum.[33] Hence, our second strategy to improve the performance of highly-ordered mesoporous TiO_2 photoanode is the top-coating of TiO_2 nanoparticles with a larger size as a light-scattering layer.

Fig. 8(a) presents a schematic diagram of a solar cell containing a novel bifunctional phothoanode, where the bottom-layer is a highly-ordered mesoporous thin film and the top-layer consists of relatively large-size light-scattering nanoparticles. Fig. 8(b) presents a cross-sectional SEM image of an optimized TiO_2 bifunctional photoanode used in the present study, which was fabricated from a highly-transparent and highly-ordered mesoporous TiO_2 bottom-layer and a Degussa P25 TiO_2 nanoparticle top-layer. The diameter of the P25 TiO_2 nanoparticles is around 20 nm, almost 2 times larger than the diameters of the nanochannels and the walls of the matrix in the mesoporous thin films. For a better comparison, the thickness of the P25 TiO_2 light-scattering layer was fixed at around 4 μm.

The photovoltaic performances of the bifunctional photoanodes in terms of increasing mesoporous TiO_2 film thickness are summarized in Table 2, together with the results on a photoanode with a single P25 layer 4 μm in thickness. Fig. 9 presents the measured *J*-*V* and IPCE curves. Interestingly, the introduction of the bifunctional photoanode in solar cells dramatically enhanced not only the conversion efficiency but also the fill factor. The solar cells with the light-scattering layer showed a ~200% higher cell efficiency than the unmodified cells in all cases. The fill factors of the solar cells with the bifunctional photoanode were higher than 0.72, while this value was around 0.5-0.6 for most of the commonly reported TiO_2 nanoparticle-based DSSCs.[2] As shown in Fig. 9(a), the solar cell with a bifunctional photoanode consisting of a 30-layer highly-ordered mesoporous TiO_2 thin film and a 4-μm P25 light-scattering top layer exhibited superior performance, with the short-circuit current (J_{sc}) 9.95 mA·cm^{-2},

the open-circuit voltage (V_{oc}) 0.72 V, the fill factor (F) 0.72, and the conversion efficiency 5.18%. We also evaluated the performance of a photoanode using only a single layer of P25 nanoparticles 4 μm in thickness as a reference. The results showed J_{sc} of 3.36 mA·cm^{-2}, V_{oc} of 0.48 V, F of 0.35, and conversion efficiency η of 1.07%. Thus, the superior performance of our bifunctional photoanode can be understood as a result of the cooperative effects of the high dye loading in the bottom mesoporous layer and the enhanced light scattering in the top layer, as well as the improved charge collection efficiency in the highly-ordered fast photon/electron transport channels.

From the viewpoint of external quantum efficiency (Fig. 5(b) and Fig. 9(b)), the IPCE of the solar cells with bifunctional photoanodes was much higher in the visible light range of 500-700 nm than for those with only either the TiO_2 mesoporous thin film or a single-layer of P25 nanoparticles. In the wavelength range below 450 nm, however, no significant change can be observed in the position of the photo-excitation peaks originating from the band-gap excitation in TiO_2 under UV light. This result demonstrates that the top-coated scattering layer can significantly enhance the light absorption in the visible light range, but has a negligible influence on the inter-band excitation of the TiO_2 photoanode. Therefore, the introduction of a scattering layer is an efficient approach to further improve the performance of photoanodes made from highly-transparent and highly-ordered mesoporous TiO_2 thin film by increasing the light absorption or the photo-electro response in the visible light regime.

Conclusions

Highly-transparent and highly-ordered TiO_2 mesoporous multilayer thin films with variable thicknesses were fabricated via an evaporation induced self-assembly method. The conversion efficiency of the highly-ordered TiO_2 thin film solar cells (0.82%) was 5 times superior to that of the transparent Solaronix photoanode solar cells (0.16%), with photoanodes of a similar thickness (approximately 1 μm).

The performance of the highly-transparent and highly-ordered TiO_2 mesoporous photoanodes was further improved by introducing either nitrogen-doping or a light-scattering top-coating layer. The N-doped TiO_2 mesoporous photoanode presented an enhancement of around 10-30% in solar cell efficiency. However, the bifunctional photoanodes consisting of a highly-ordered TiO_2 mesoporous bottom layer and a Degussa P25 light-scattering top layer presented a more significant improvement in photon-to-current conversion efficiency. There was a ~200% enhancement in the cell efficiency compared to the unmodified cells and a high fill factor beyond 0.72, owing to the higher dye adsorption, better light scattering, and faster photon/electron transportation of the bifunctional photoanode. The performance enhancement realized by the bifunctional photoanodes, which combine the merits of highly-ordered mesoporous TiO_2 thin films and light-scattering TiO_2 nanoparticles, demonstrates the success of our strategies for improving the performance of DSSCs.

Acknowledgments

This work was supported by Australian Research Council Discovery Project DP1096546. ZQS was supported by an Australian Postdoctoral Research (APD) Fellowship. The authors also are grateful for experimental assistance from Drs Ivan P. Nevirkovets, Darren Attard, Germanas Peleckis, Dongqi Shi, and Wenxian Li. The authors also thank Dr. Tania Silver for her critical reading of this manuscript.

Notes and references

[a] *Institute for Superconducting & Electronic Materials, University of Wollongong, Innovation Campus, Squires Way, North Wollongong, NSW 2500, Australia . Fax: +61-2-4221-5731; Tel: +61-2-4298-1420; E-mail: jhk@uow.edu.au.*

1 B. O'Regan, M. Grätzel, *Nature*, 1991, **353**, 737.
2 A. Hagfeldt, G. Boschloo, L. Sun, L. Kloo and H. Pettersson, *Chem. Rev.*, 2010, **110**, 6595.
3 Z. Q. Sun, J. H. Kim, Y. Zhao, F. Bijarbooneh, V. Malgras, Y. Lee, Y. M. Kang and S. X. Dou, *J. Am. Chem. Soc.*, 2011, **133**, 19314.
4 X. Chen and S. S. Mao, *Chem. Rev.*, 2007, **107**, 2891.
5 J. C. Brendel, Y. Lu and M. Thelakkat, *J. Mater. Chem.*, 2010, **20**, 7255.
6 Z. Liu, Y. Li, Z. Zhao, Y. Cui, K. Hara and M. Miyauchi, *J. Mater. Chem.*, 2010, **20**, 492.
7 S. Guldin, S. Huttner, P. Tiwana, M. C. Orilall, B. Ulgut, M. Stefik, P. Docampo, M. Kolle, G. Divitini, C. Ducati, S. A. T. Redfern, H. J. Snaith, U. Wiesner, D. Eder and U. Steiner, *Energy Environ. Sci.*, 2011, **4**, 225.
8 W. Wang, T. Higuchi, M. Suzuki, T. Fukuoka, T. Shimomura, M. Ono, L. Radhakrishnan, H. Wang, N. Suzuki, H. Oveisi, and Y. Yamauchi, *Angew. Chem. Int. Ed.*, 2010, **49**, 3956.
9 M. Zukalova, A. Zukal, L. Kavan, M. K. Nazeeruddin, P. Liska, and M. Graetzel, *Nano Letters*, 2005, **5**, 1789.
10 K. Hou, B. Tian, F. Li, Z. Bian, D. Zhao, C. Huang, *J. Mater. Chem.*, 2005, **15**, 2414.
11 W. Chen, X. Sun, Q. Cai, D. Weng, H. Li, *Electrochem. Commun.*, 2007, **9** 382.
12 M. Wei, Y. Konishi, H. Zhou, M. Yanagida, H. Sugihara and H. Arakawa, *J. Mater. Chem.*, 2006, **16**, 1287.
13 W. Han and Z. Lin, *Angew. Chem. Int. Ed.*, 2012, **51**, 1534.
14 X. Xin, M. He, W. Han, J. Jung, and Z. Lin, *Angew. Chem. Int. Ed.*, 2011, **50**, 11739.
15 M. He, F. Qiu, and Z. Lin, *J. Mater. Chem.*, 2011, **21**, 17039.
16 W. Han, M. Byun, L. Zhao, and Z. Lin, *J. Mater. Chem.*, 2011, **21**, 14248.
17 M. Zukalova, J. Prochazka, A. Zukal, J. H. Yum, and L. Kavan, *Inorgan. Chim. Acta*, 2008, **361**, 656.
18 N. Satoh, T. Nakashima, K. Kamikura, and K. Yamamoto, *Nature Technology*, 2008, **3**, 106.
19 V. Swamy, B. C. Muddle, and Q. Dai, *Appl. Phys. Lett.*, 2006, **89**, 163118.
20 M. D. Earle, *Phys. Rev.*, 1942, **61**, 56.
21 E. M. Barea, M. Shalom, S. Gimenez, I. Hod, I. Mora-Sero, A. Zaban, and J. Bisquert, *J. Am. Chem. Soc.*, 2010, **132**, 6834.
22 C. Burda, Y. Lou, X. Chen, A. C. S. Samia, J. Stout and J. L. Gole, *Nano Lett.*, 2003, **3**, 1049.
23 H. Tian, L. Hu, C. Zhang, S. Chen, J. Sheng, L. Mo, W. Liu and S. Dai, *J. Mater. Chem.*, 2011, **21**, 863.
24 J. Wang, D. N. Tafen, J. P. Lewis, Z. Hong, A. Manivannan, M. Li, and N. Wu, *J. Am. Chem. Soc.*, 2009, **131**, 12290.
25 G. Liu, L. Wang, H. Yang, H. Cheng and G. Lu, *J. Mater. Chem.*, 2010, **20**, 831.
26 G. Gohin, I. Maurin, T. Gacoin and J. Boilot, *J. Mater. Chem.*, 2010, **20**, 8070.
27 T. Ma, M. Akiyama, E. Abe and I. Imai, *Nano Lett.*, 2005, **5**, 2543.
28 R. Asahi, T. Morikawa, T. Ohiwaki, K. Aoki and Y. Taga, *Science*, 2001, **293**, 269.
29 H. Irie, S. Watanabe, K. Hashimoto, *J. Phys. Chem. B*, 2003, **107**, 5483.

30 O. Diwald, T. L. Thompson, E. G. Goralski, S. D. Walck, J. K. Yates Jr., *J. Phys. Chem. B*, 2004, **108**, 6004.
31 Z. Zhou and Y. Huang, *J. Phys.: Conf. Ser.*, 2009, **188**, 012033.
32 M. Gratzel, *Inorg. Chem.*, 2005, **44**, **6841**.
33 Y. Qiu, W. Chen, and S. Yang, *Angew. Chem. Int. Ed.*, 2010, **49**, 3675.
34 S. Ito, S. M. Zakeeruddin, R. Humphty-Baker, P. Liska, R. Charvet, *Adv. Mater.*, 2006, **18**, 1202.
35 H. Koo, Y. J. Kim, Y. H. Lee, W. I. Lee, K. Kim, and N. G. Park, *Adv. Mater.*, 2008, **20**, 195.